The Compass: Earth Science Journal of Sigma Gamma Epsilon

Volume 85 | Issue 3 Article 2

11-12-2013

Timing of Thermal Overprints in the Silvermines Granite and Associated Diabase Intrusions, St. Francois Mountains, Missouri

Renee C. Rohs
Northwest Missouri State University, rrohs@nwmissouri.edu

Timing of Thermal Overprints in the Silvermines Granite and Associated Diabase Intrusions, St. Francois Mountains, Missouri

Renee C. Rohs
Department of Natural Sciences
Northwest Missouri State University
800 University Drive
Maryville, MO 64468 USA
rrohs@nwmissouri.edu

ABSTRACT

Igneous rocks exposed in the St. Francois Mountains record the geologic history of volcanic activity and plutonic intrusions contributing to the growth and stabilization of the continental crust during the Precambrian. These igneous rocks also contain evidence of thermal overprinting both in the isotope chemistry and the crystalline structures. This study presents new isotopic, mineral and petrologic data to support the timing of dike emplacement and thermal overprinting in the host rock. The study area for this research is along the East Fork of the St. Francis River at the Silver Mines Recreation Area where diabase dikes intrude the surrounding granite. Samples of the Silvermines granite and diabase were collected for petrologic study and isotopic analyses. Thin section analyses revealed minerals and textures that suggest magmatic segregation as well as thermal variation in the diabase intrusions. The surrounding granite exhibits thermal alteration at the contact with the diabase. X-ray diffraction patterns support the thin section analyses and provide clarification on opaque minerals. An x-ray diffraction pattern for the granite also indicates orthoclase, supporting existing data sets for structural resetting of K-feldspar in both the volcanic and plutonic rocks in the area. Mineral separates were prepared for granite samples at the contact with the diabase and at a distance of 10 m from the contact. Gas ages were determined using Ar-Ar methodologies for the diabase groundmass as well as K-feldspar, biotite, and amphibole in the host granite. According to the Ar-Ar data collected, the total gas age for the diabase is 1167.1 ± 7.9 Ma. Ar-Ar data from the granite is more complex indicating Precambrian timing with total gas ages of 904, 1066, 1119, and 1258 Ma. Based on this information, it is evident that a significant thermal event altered the Silvermines granite as early as 1258 Ma to as late as 904 Ma. This thermal event may be associated with the intrusion of the Silver Mines dike swarm and its magmatic source.

KEY WORDS: Precambrian, isotope chemistry, Silver Mines Recreation area, diabase dikes, Eastern Granite and Rhyolite (EGR) province, Skrainka mafic group, Silver Mines mafic group, Butler Hill Granite, Slabtown Granite

INTRODUCTION

The purpose of this study is to examine the relationship between the Silvermines Granite and the mafic dike swarm that intrudes the Precambrian granite. This relationship includes the nature and timing of the dike emplacement as well as the effect on the surrounding granite. In addressing the purpose of this study, there are three distinct goals. The first goal is to establish the mineralogy and petrology of the intruding dikes. The second goal is to establish the timing of intrusion for the dikes. With a firm understanding of the dike intrusions, the third goal is to examine the thermal impact of the dike intrusions on the surrounding granite.

Basement rock units exposed in the St. Francois Mountains (fig. 1) are part of the Eastern Granite and Rhyolite (EGR) province, representing a major pulse of continental growth during the Meso-proterozoic at approximately 1470 Ma (Van Schmus et al., 1987; 1993; and Lidiak et al., 1993). Exposures of the Precambrian basement in the St. Francois Mountains, provide a window in the continental crust showing composition and configuration (Rohs, 2003).

Most of the volcanic units within the St. Francois Mountains have been attributed to large-scale, caldera-type volcanism with several volcanic centers (Kisvarsanyi, 1981). Several different granitic plutons have been recognized as forming in rings where magma intruded after structural collapse of the large calderas (Kisvarsanyi, 1981). One of these ring plutons, the Silvermines granite, is dated at 1484 Ma (Bickford et al., 1981) and is exposed along the St. Francois River at Silver Mines. Isotopic dating of the other ring plutons has yielded similar ages near the overall age of 1470 Ma for the province (Van Schmus et al., 1993). However, two other granite bodies within the St. Francois Mountains, the Graniteville and Munger plutons, have been dated at 1357 Ma (Van Schmus et al., 1996) and 1378 Ma (Thomas et al., 1984) respectively. These plutons are similar in age to the Southern Granite and Rhyolite (SGR) province to the west at approximately 1370 Ma (Van Schmus et al., 1987; 1993; 1996 and Barnes et al. 1999).

Mafic rocks in the St. Francois Mountains occur as dikes and sills. Two groups of mafic rocks, Silver Mines and Skrainka, have been recognized based on similarities in geochemical signatures (Sylvester, 1984). A gabbroic sill within the Skrainka group has been dated at approximately 1316 Ma (Rämö and others, 1994) and therefore post-dates the silicic magmatism in the area. Mafic intrusions of the Silver Mines group have been interpreted as occurring at approximately the same time as silicic volcanism and plutonic emplacement based on compositional similarities with a mafic volcanic flow occurring between felsic units exposed at Johnson's Shut-Ins state park (Sylvester, 1984). Sm-Nd isotopic data also support this interpretation with depleted mantle model ages of 1.43-1.54 Ga for diabase samples in the area and 1.52-1.55 Ga for the Silvermines Granite and a trachyte within the province (Rohs and Van Schmus, 2007).

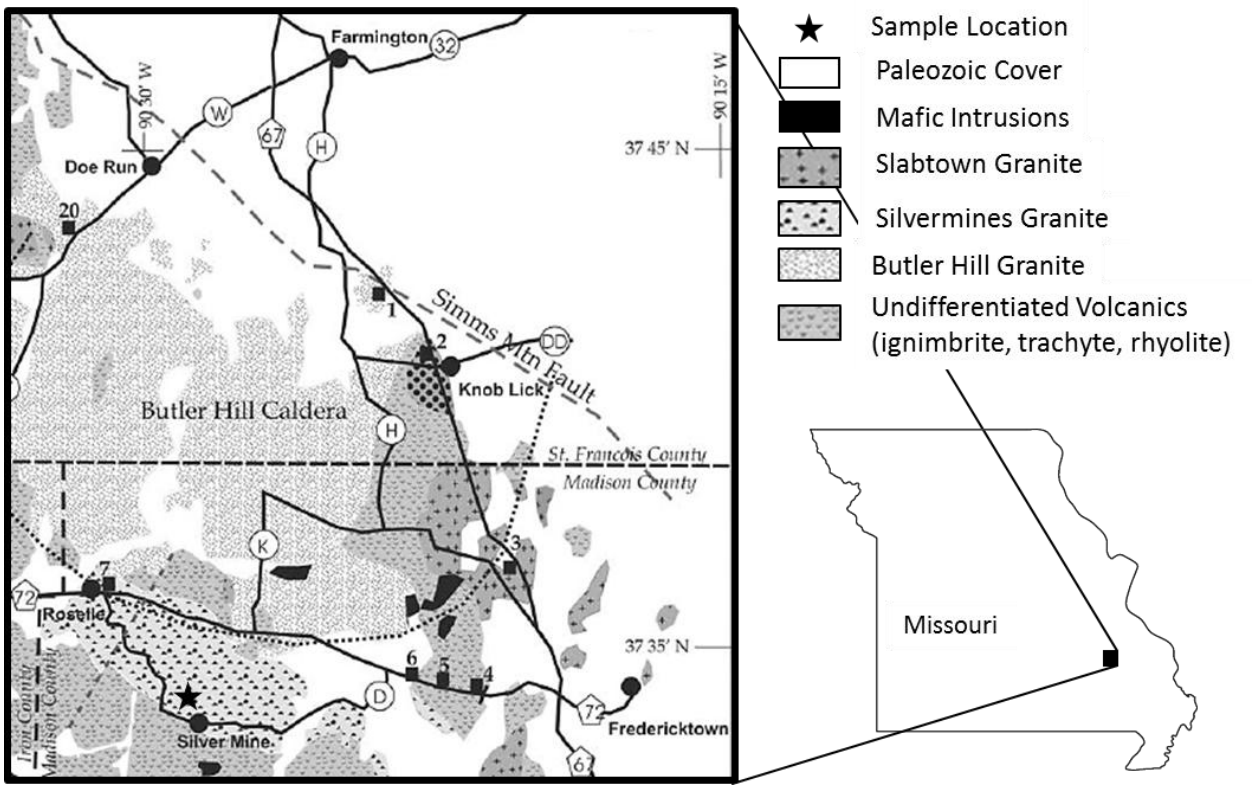

Figure 1. General geologic map of the Butler Hill Caldera in the St. Francois Mountains showing sample locations as modified from Meert and Stuckey, 2002.

METHODS

Sample collection and preparation

Hand samples were collected from the large diabase dike intruding the Silvermines Granite along the St. Francois River at Silver Mines (fig. 2). Several samples were collected across the width of the dike to study petrographic changes from the chill margin to the interior of the dike. Additional samples were collected at several other dike intrusions along the St. Francois River between the Silver Mines recreation area and the Tiemann Shut-Ins area upstream (Aldieri *et al*., 2010). Finally, samples were collected from the granite at the contact with the dike intrusion and at a distance of 30 m from the dike intrusions. Selected samples were chosen for thin section analyses, X-ray diffraction, and isotopic analyses.

Thin Section Analysis

Several samples were selected for thin section analysis to determine the mineral content and textural differences. The thin sections were examined using a petrographic microscope under plane polarized light (PPL) and cross polarized light (XPL) viewed at 40x and 100x magnification. Textural differences were most easily recognized in PPL due to the abundance of opaque minerals in the mafic dike samples. Individual mineral relief and textures were also apparent in PPL including

Figure 2. Silvermines diabase dike at Silver Mines

Thin Section Analysis

Several samples were selected for thin section analysis to determine the mineral content and textural differences. The thin sections were examined using a petrographic microscope under plane polarized light (PPL) and cross polarized light (XPL) viewed at 40x and 100x magnification. Textural differences were most easily recognized in PPL due to the abundance of opaque minerals in the mafic dike samples. Individual mineral relief and textures were also apparent in PPL including euhedral to anhedral crystal forms as well as crystal habit. In XPL, the extinction angles of feldspars were used to determine the range of composition as An content based on the Michel-Levy method for plagioclase. Twinning patterns in K-feldspars were used to identify microcline apart from orthoclase. Interference colors and mineral cleavage or fracture aided in the identification of calcite apart from quartz and pyroxene.

XRD Analysis

A couple of the samples were prepared for mineral analysis using x-ray diffraction. The samples were crushed and sieved to a size smaller than 63μm. The samples were analyzed using a Cu anode in the Miniflex X-ray diffractometer with continuous collection between 2θ angles of 5 and 70°. Background noise and kα2 interference were removed from the diffraction patterns prior to peak analysis. Peak locations and intensity were compared with powder diffraction files for known minerals for mineral composition.

U-Pb Isotopic Analyses

Prior to isotopic analysis, zircon crystals were separated into magnetic fractions, chosen for clarity, and abraded. Individual crystals were placed in a solution of HF/HNO_3 followed by HCl for dissolution. After dissolution a $^{205}Pb/^{325}U$ tracer was added prior to analysis. Analyses were completed at the University of Kansas Isotope Geochemistry Laboratory using a VG Sector thermal ionization mass spectrometer with ion-counting Daly multiplier for isotopic ratios in the samples. The decay constant of $0.155125x10^{-9}$/year was used for ^{238}U for and $0.98485x10^{-9}$/year for ^{235}U (Steiger and Jaiger, 1977). See Rohs and Van Schmus (2007) for additional information on procedures.

Ar-Ar Isotopic Analyses

Three samples were selected for Ar-Ar isotopic analyses including the large diabase intrusion at Silver Mines, the Silvermines granite in contact with the diabase, and the granite at a distance of 30 m from the contact with the diabase. These samples were prepared for groundmass and mineral separates at the Nevada Isotope Geochronology Laboratory including K-feldspar, amphibole, and biotite. The samples were run as conventional furnace step heating analyses to produce an apparent age spectrum. This age spectrum assumes that the non-radiogenic argon is at atmospheric levels with $^{40}Ar/^{36}Ar = 295.5$. If the ratio between these two isotopes of Ar is greater than 295.5, the excess ^{40}Ar will produce an older age and manifest itself as a U-shaped spectra shape. Total gas ages using $^{40}Ar/^{39}Ar$ are equivalent to K/Ar and represent the primary data used in this study since isochrones were not obtained and the samples did not yield significant plateaus during analysis.

RESULTS

Mineralogy and Petrology

The mineral content and textures in the diabase dikes are quite variable as shown in Figures 3a-c, 4. In nearly all of the diabase samples, the primary mineral was plagioclase. In the large dike at Silver Mines, plagioclase occurs in lath-shaped crystals with a composition of An_{45-55} as determined by the Michel-Lévy method using extinction angles for a low-temperature igneous rock (Tobi and Kroll, 1975). Plagioclase makes up approximately 60-70% of the minerals contained within the diabase. The next most abundant mineral based on thin section analyses of the diabase intrusions, is magnetite. Magnetite typically occurs as euhedral or subhedral crystals within most thin sections of the diabase. Several minerals could be identified in thin section including quartz, calcite, ilmenite or hematite, olivine, and pyrite. Other minerals occurred as fine crystals or as alteration products including serpentine, sericite, and chlorite.

Mineralogy of the diabase was also determined by XRD and is shown in Figure 5. Peak location and intensity were used to identify andesine as the plagioclase variety present in the sample. Magnetite and calcite have also been identified as specific peaks

within the powder diffraction pattern. Two additional silicate minerals, low quartz and antigorite serpentine, were indicated in the sample based on statistical matching of the diffraction pattern with known minerals.

Texture within the large diabase exhibited a gradual increase in grain size from the chill margin to the center of the dike as shown in Figure 3. Spherical structures ranging from 0.5-1.0 mm in diameter occur within the diabase (Figure 4a and b) and are more prevalent in some areas compared with others. The spherical structures are typically rimmed with euhedral crystals of magnetite.

The occurrence of these spherical structures is somewhat variable. They are found throughout the large dike and in several of the smaller dikes as well. They can occur alone or in clusters. Mineralogy and texture within the spherical structures tend to fall into three categories. The first group has a distinct sphere of calcite in the interior and anhedral sulfide bodies within the calcite. The sulfide bodies are opaque in transmitted light but a brassy-gold color in reflected light. A second group of these spherical structures have silicates and oxides as fine-grained aggregates within the spheres. Mineralogy within the second group appears to be plagioclase and ilmenite or hematite. The third type of spherical structure is an aggregate of magnetite crystals and appears opaque in thin section (Aldeiri *et al*., 2010).

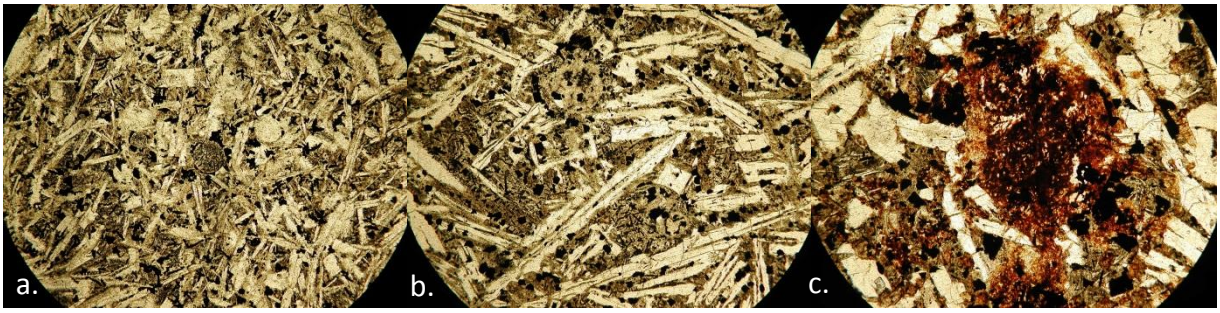

Figure 3a-c. Photomicrographs from the chill margin on the left to the center of the dike on the right showing the change in grain size. All photomicrographs have a viewing field of 4.5 mm across.

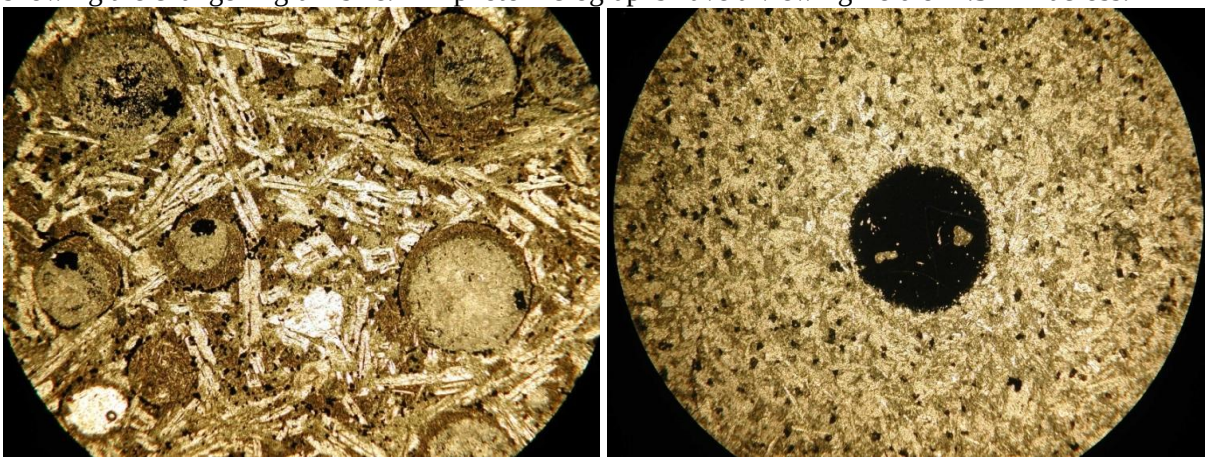

Figure 4a and b. Spherical structures in diabase samples as shown in plane-polarized light. The extent of the viewing field is 4.5 mm. Photomicrograph 4b. from Barnes, *et al.*, 2010.

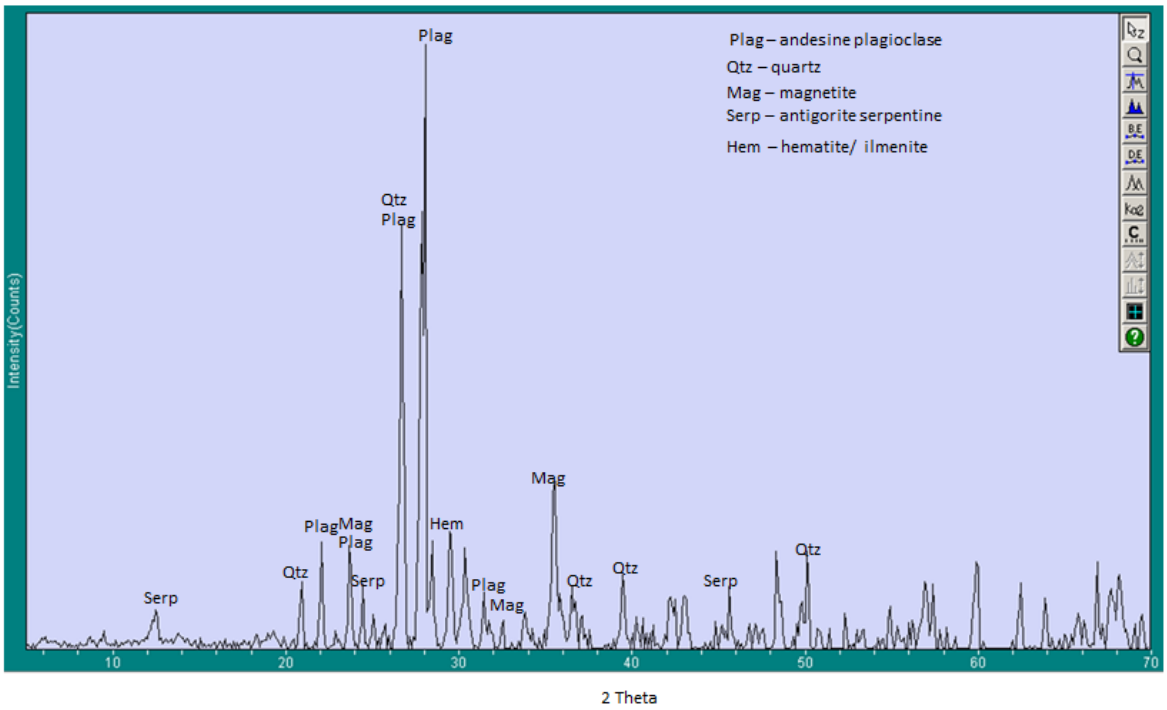

Figure 5. Interpreted XRD powder diffraction file for Silvermines diabase.

Isotopic Ages

Isotopic ages were determined for several samples collected from the Silvermines Granite and intrusive diabase dikes. The resulting data exhibits an age range from 1473 to 960 Ma depending on the isotopic system and minerals analyzed. Isotopic data are given in Tables 1 and 2 (at end of paper). Zircons collected from the large diabase dike were analyzed for U-Pb ages. Three zircon fractions were analyzed for U-Pb isotopic composition and ages were calculated. Two of the zircon fractions resulted in $^{207*}Pb/^{206*}Pb$ ages of 1473 and 1477 Ma. Using these two zircons, a concordia plot was constructed as shown in Figure 6 with an intercept age of 1474±7 Ma. The other zircon fraction was reversely discordant and anomalous with a $^{206*}Pb/^{238}U$ age of 339 Ma. Therefore, the two previous zircon fractions were used to construct a concordia plot shown in Figure 6 with an intercept age of 1474±7 Ma.

Ar-Ar isotopic data varied depending on the rock type, minerals analyzed and relative distance. A sample of the groundmass from the large diabase dike at Silver Mines was analyzed and produced a moderately discordant age spectrum, with ages that progressively increased from an initial step of ~713 Ma to a "plateau like" segment (steps 5-8) at ~1200-1280 Ma, followed by decreasing ages with the last ~20% gas released. The total gas age of the diabase is 1167.3 ± 7.9 Ma, and there were no plateau or isochron ages defined for the diabase as shown in Figure 7a.

A sample of K-feldspar from the Silvermines Granite at the contact with the diabase displays a very discordant age

spectrum, with numerous features which suggest the presence of alteration and excess argon. The age spectrum begins with high, and variable ages, which decrease until ~45% gas released. From ~45-80% gas released the sample exhibits progressively increasing ages, after which the ages decrease and then increase dramatically for the final ~15% gas released. The total gas age is 1259.0± 8.6 Ma. There were no plateau or isochron ages defined for this sample. The initial ~8 steps, all at temperatures <600 ^{o}C, comprise an unusually large amount of gas release (~29%) for a K-feldspar as shown in Figure 7b. In comparison, amphibole from the same sample produced a mildly discordant (i.e. mostly flat) age spectrum with most steps around 960 Ma. The total gas age for the amphibole in the granite at the contact is 904.8 ± 8.2 Ma (Figure 7c).

Finally, both biotite and K-feldspar were analyzed in a sample of the Silvermines Granite at a distance of ~10 m from the contact with the diabase. The biotite sample yielded a highly disturbed, discordant age spectrum (Figure 7d). Ages decrease from an initial step of ~1098 Ma to ~525 Ma for the second step, followed by generally increasing ages for steps 3-9. The total gas age of the biotite is 1066.0 ± 7.8 Ma. Aside from evidence for excess argon in the first ~10% gas released for the K-feldspar, the sample produced an age spectrum which is very likely to be useful for multi-domain modeling with a total gas age of 1119.3 ± 7.5 Ma (Figure 7e).

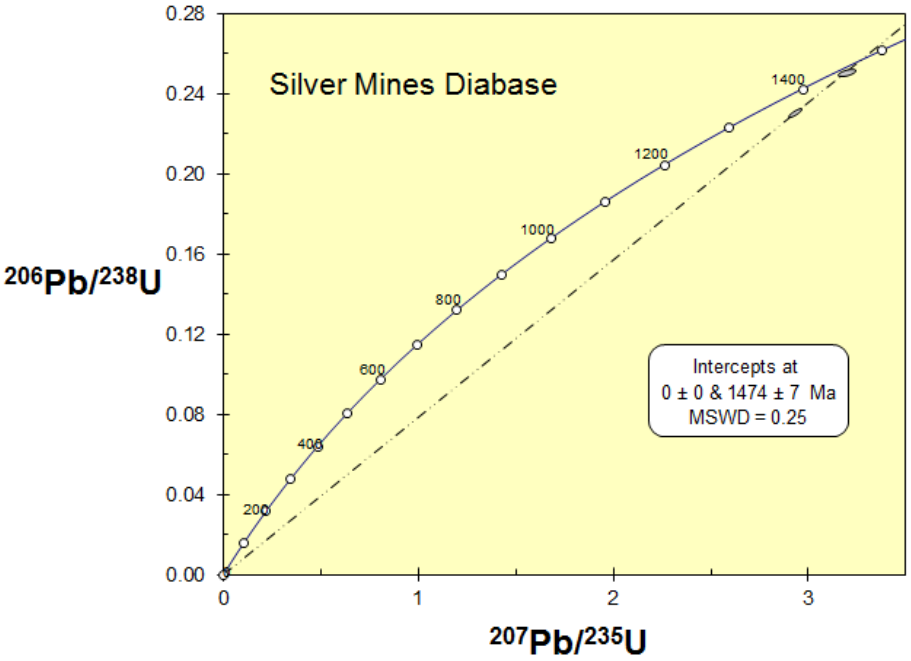

Figure 6. Concordia plot for zircons from Silvermines diabase.

Figures 7a-e. Age spectrums for Ar gas release for a. diabase, b. K-feldspar at the contact, c. amphibole, d. biotite, and e. K-feldspar at ~10 m from the contact.

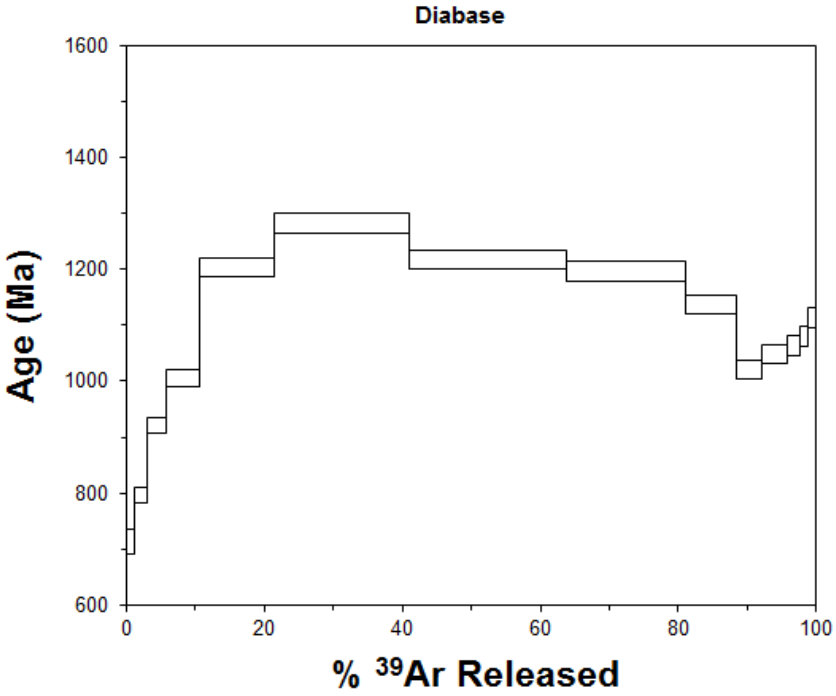

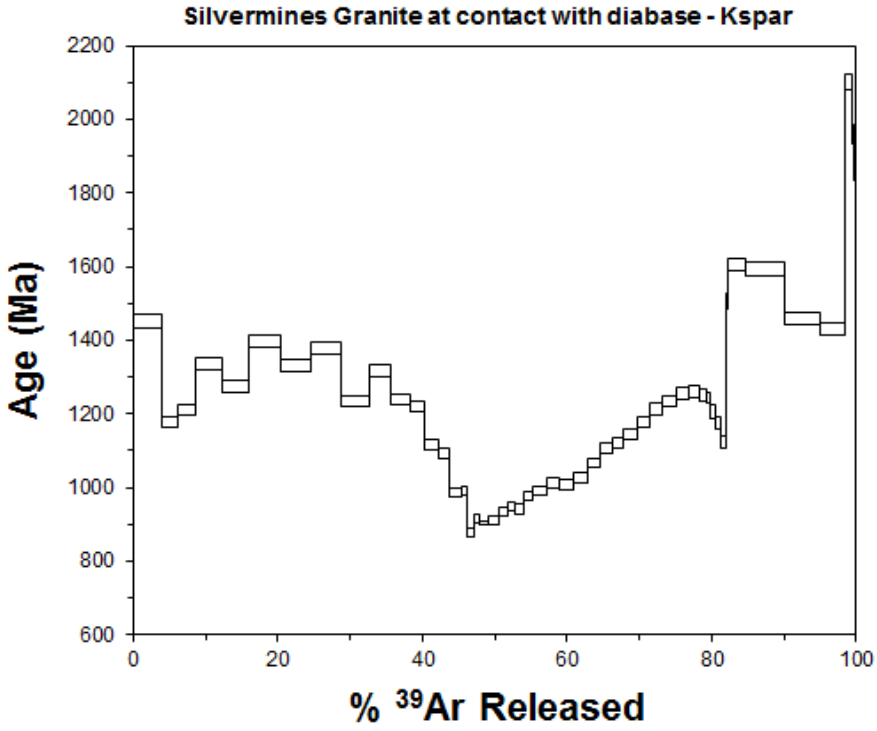

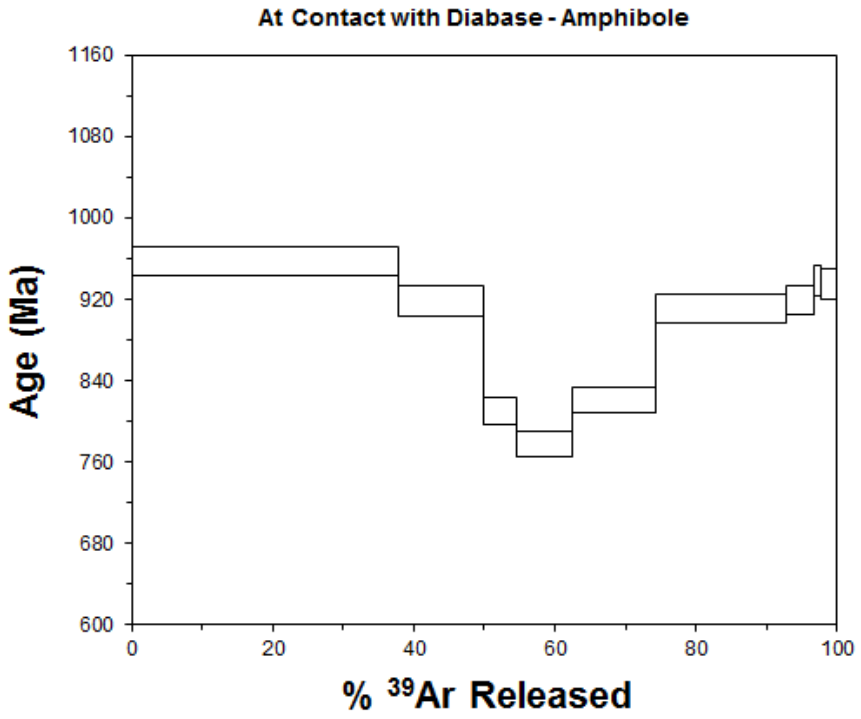
At Contact with Diabase - Amphibole
Age (Ma)
1160
1080
1000
920
840
760
680
600
0
20
40
60
80
100
% 39Ar Released

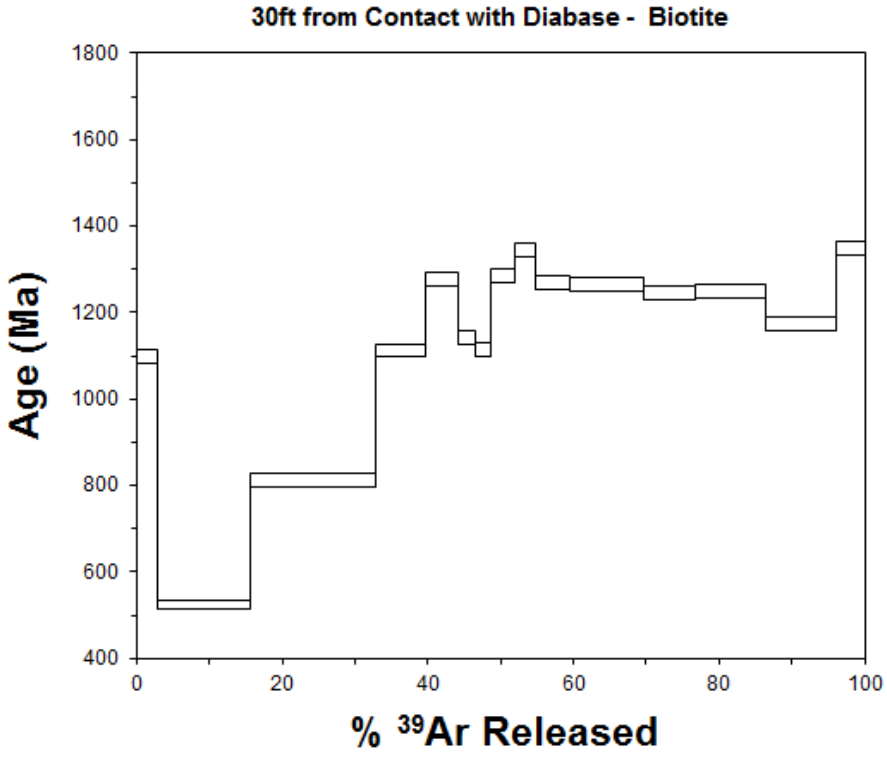
30ft from Contact with Diabase - Biotite
Age (Ma)
1800
1600
1400
1200
1000
800
600
400
0
20
40
60
80
100
% 39Ar Released

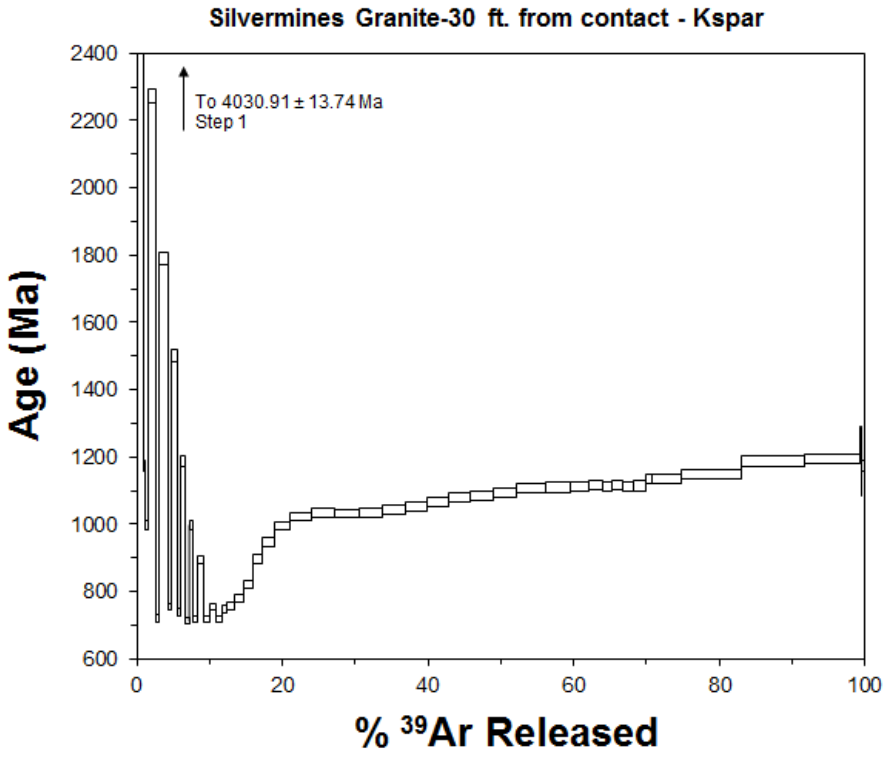

DISCUSSION

The mineralogy of the diabase dikes supports the interpretation of mafic to ultramafic composition. Although the individual dikes vary in mineralogical mode, the primary minerals are plagioclase and magnetite. There is significant evidence of alteration with the presence of serpentine, chlorite and sericite in the groundmass of the diabase samples. The spherical features are the most unusual features of these samples. Information from the thin section analyses supports the presence of calcite and sulfide minerals within spherical structures. Because these structures are separate from calcite veins, they most likely represent segregation vesicles. Based on the texture and mineral layout within the segregation vesicles, they are interpreted as immiscible liquid droplets that crystallized during the original emplacement of the diabase dike. The occurrence of magnetite around the outside of these structures implies that they acted as a nucleation surface for the magnetite. The calcite within the segregation vesicles is fine grained and does not contain void spaces as expected during secondary filling of void spaces. Opaque minerals in the spherical structures include pyrite and ilmenite. For example, the pyrite is found within the calcite while ilmenite occurs with fine plagioclase laths. The ilmenite is concentrated within the spherical structures but does occur elsewhere in the finer matrix between plagioclase laths in the mass of the rock.

The large diabase dike at Silver Mines has been previously recognized as part of the Silver Mines dike swarm

(Sylvester, 1984, Walker, *et al*., 2002). These intrusive structures along with a mafic volcanic flow exposed along the Black River at Johnson's Shut-Ins, have been linked to one another geochemically (Sylvester, 1984). As a result, the Silver Mines dike swarm has been interpreted as forming shortly after the emplacement of the Silvermines granite (Sylvester, 1984 and Walker, *et al*. 2002) at 1484 Ma (Van Schmus, *et al.,* 1993). Data from this study supports this interpretation suggesting that the diabase dikes were emplaced as early as 1474 Ma. However, since zircons are not commonly found in diabase, it is possible that the zircons are xenocrysts from the surrounding granite. If that is the case, then the Ar-Ar age for the diabase groundmass could be interpreted as the minimum age of intrusion at 1167 Ma.

Studies of the structural state of K-feldspar in the St. Francois Mountains suggest a large-scale thermal event that reset both the plutonic and volcanic felsic rocks within the area (Plymate, *et al.*, 2001, 1992, Collins and Rohs, 2004). Based on the Ar-Ar data from the Silvermines Granite, there is evidence for at least one event of thermal disruption. Thermal resetting may have taken place around 1240 Ma as indicated by a plateau-like region of the diabase and the total gas age of K-feldspar at the contact with the diabase. On a regional level, the Grenville Orogeny was taking place during this time to the east but the volcanic and plutonic units in the study area are undeformed (Lidiak, *et al.,* 1993). The highly discordant spectrum associated with the K-feldspar at the contact with the diabase provides limited interpretation. However, the K-feldspar at a distance of ~10 m from the diabase is much more reliable and indicates a total gas age of approximately 1119 Ma. This age is similar to the total gas age of the diabase at 1167. These ages roughly correspond to the beginning stages of the Midcontinent Rift system (Van Schmus and Hinze, 1993) to the north and west of the study area. The thermal upwelling associated with the opening of the Midcontinent Rift may have been sufficient to thermally reset the rocks in the area though this should be evident throughout plutonic and volcanic rocks of the Eastern Granite and Rhyolite province if this is the case.

In conclusion, there appears to be evidence of a mafic magmatic event in which a number of diabase dikes intruded the granite and rhyolite units exposed near the Silver Mines Recreation area in southeast Missouri. This mafic magmatic event exhibits evidence of immiscible magmas enriched in magnetite, calcite, and sulfides. These mafic intrusions may have been emplaced as early as 1474 Ma or as late as 1167 Ma. If the magmatism occurred at the more recent age, it may have been associated with the structural resetting of K-feldspar within the region. If the magmatism was earlier, then the diabase, K-feldspar, and biotite all show evidence of a major thermal event around 1120±50 Ma. In any case, the Ar-Ar data presented here supports the evidence of earlier studies suggesting a thermal overprint in the igneous rocks of the St. Francois Mountains.

ACKNOWLEDGEMENTS

This research was supported by a number of Applied Research Grants and Undergraduate Research Grants provided by Northwest Missouri State University through the Faculty Research Committee, Dr. Charles McAdams – Dean of the College of Arts and Science, and Dr. Gregory Haddock – Vice Provost. I would like to thank Dr. W.R. (Randy) Van Schmus and the Isotope Geology Laboratory at the University of Kansas for preparing and analyzing zircon samples for U-Pb isotopic data as well as informative discussions at many points along the way. I would also like to thank Dr. Terry Spell and Kathleen Zanetti at the Nevada Isotope Geochronology Laboratory for preparing and analyzing mineral and rock samples for Ar-Ar isotopic data. Finally, a special thanks to all of those undergraduate students who have worked with me on this project collecting, cutting, and crushing rock samples including Rachael Collins, Allen Anderson, and Kati Tomlin.

REFERENCES CITED

Aldieri, M., Johnson, A. W. and Rohs, C. R., 2010, Petrology of the non-felsic rocks associated with the Silvermines Granite. GSA Abstracts with Programs, Vol. 42, No. 2.

Barnes, M.A., Rohs, C.R., Anthony, E.Y., Van Schmus, W.R., and Denison, R.E., 1999, Isotopic and elemental chemistry of subsurface Precambrian igneous rocks, west Texas and New Mexico: Rocky Mountain Geology, v. 34, no. 2, p. 245-262.

Bickford, M.E., Harrower, K.L., Hoppe, W.J., Nelson, B.K., Nusbaum, R. L., and Thomas, J.J., 1981. Rb-Sr and U-Pb geochronology and distribution of rock types in the Precambrian basement of Missouri and Kansas. Geological Society of American Bulletin. 92, 323-341.

Collins, R. D. and Rohs, C.R., 2004, Mineralogy of granite and rhyolite units in the St. Francois Mountains. GSA Abstracts with Programs, v.36, n. 2.

Kisvarsanyi, E.B., 1981, Geology of the Precambrian St. Francois terrane, Southeastern Missouri: Contributions to Precambrian Geology, v. 64, n. 8, 58p.

Lidiak, E.G., Bickford, M.E., and Kisvarsanyi, E.B., 1993. Proterozoic geology of the eastern midcontinent region, in Reed, J.C., Jr., and six others, eds., Precambrian: Conterminous U.S.: Boulder, Colorado, Geological Society of America, Geology of North America v. C-2, pp. 270-281.

Meert, J.G. and Stuckey, W., 2002. Revisiting the paleomagnetism of the 1.476 Ga St.Francois Mountains igneous province, Missouri. Tectonics v. 21 n. 2, p. 1007

Plymate, T.G., Kendall, J.D., Shepard, L.M. and Clark, K.C., 2001. Structural state of K-feldspar in the felsic volcanic rocks and ring pluton granites of the Butler Hill Caldera, St. Francois Mountains,southeastern Missouri; Can Mineral v. 39, p. 73-83

Plymate, T.G., Daniel, C.G., and Cavaleri, M.E., 1992. Structural state of K-feldspar in the Butler Hill-Breadtray Granite, St. Francois Mountains, southeastern Missouri; Can Mineral v. 3, p. 367-376

Rämö, O.T., Boyd, W.W., Vaaskoki, M., Cameron, R.L., and Ryckman, D.A., 1994, 1.3 Ga mafic magmatism of the St. Francois Mountains of SE Missouri., implications for mantle composition beneath mid-continental USA: Miner. Mag. 58A, 754-755.

Rohs, C.R., 2001. Identifying Paleoproterozoic and Meso-proterozoic crustal domains within the Southern Granite and Rhyolite province, mid-continent North America, Ph.D. thesis, University of Kansas.

Rohs, C. R., 2003. Mafic intrusions in the St. Francois Mountains of Southeast Missouri: A study of the petrology, geochemistry, geochronology, and tectonic emplacement. GSA Abstracts with Programs, v. 35, n. 2

Rohs, C.R. and W.R. Van Schmus, 2007. Isotopic connections between basement rocks exposed in the St. Francois Mountains and the Arbuckle Mountains, southern mid-continent, North America. International Journal of Earth Sciences, v. 96, p. 599-611.

Steiger R.H. and Jaiger, E., 1977, Subcommission on geochronology convention on the use of decay constants in geo- and cosmochromonology. Earth Planetary Science Letters, v. 36, p. 359-362.

Sylvester, P.J., 1984, Geology, petrology, and tectonic setting of the mafic rocks of the 1480 Ma old granite-rhyolite terrane of Missouri, USA; Thesis (Ph.D.) Washington University, Dept. of Earth and Planetary Sciences, 455 p.

Tobi, A.C. and Kroll, H., 1975, Optical determination of the An-content of plagioclases twinned by the Carlsbad-law: A revised chart: American Journal of Science, v. 275, p. 731-736.

Thomas, J.J., Shuster, R.D., and Bickford, M.E., 1984. A terrane of 1350- to 1400-m.y.-old silicic volcanic and plutonic rocks in the buried Proterozoic of the mid-continent and in the Wet Mountains, Colorado. Geological Society of America Bulletin. 95, 1150-1157.

Van Schmus, W.R., Bickford, M.E., and Zetiz, I., 1987. Early and middle Proterozoic provinces in the Central United States: Proterozoic Lithospheric Evolution AGU Geodynamics Series, v.17, pp. 43-68.

Van Schmus, W.R., Bickford, M.E., Sims, P.K., Anderson, R.R., Shearer, C.K., and Treves, S.B., 1993. Proterozoic geology of western midcontinent basement, in Reed, J.C., Jr., and six others, eds., Precambrian: Conterminous U.S.: Boulder, Colorado, Geological Society of America, Geology of North America v. C-2, pp. 239-259.

Van Schmus, W.R., and Hinze. 1993 Midcontinent Rift System, in Reed, J.C., Jr., and six others, eds., Precambrian: Conterminous U.S.: Boulder, Colorado, Geological Society of America, Geology of North America v. C-2, pp. 292-303.

Van Schmus, W.R., Bickford, M.E., and Turek, A., 1996. Proterozoic geology of the east-central Midcontinent basement. GSA Special Paper 308, 7-32.

Walker, J.A., Pippin, C.G., Cameron, B.I., and Patino, L., 2002, Tectonic insights provided by Meso-proterozoic mafic rocks of the St. Francois Mountains, southeastern Missouri.

Table 1. U-Pb Isotopic Data and Ages

Isoplot Data	**Size**	**U**	**Pb**	$\frac{Pb^{206}}{Pb^{204}}$	$\frac{Pb^{207*}}{U^{235}}$	**±2σ**	$\frac{Pb^{206*}}{U^{238}}$	**±2σ**	**Correl. Coeff.**
Sample	**(mg)**	**ppm**	**ppm**	**(obs.)**		**(pct)**		**(pct)**	**(rho)**
SFM-1V3	0.001	307	78	1361	2.9293	0.83	0.23028	0.69	0.864
SFM-1V1a	0.005	132	39	690	3.1933	1.10	0.25043	0.63	0.609
SFM-1V4	*0.001*	*870*	*48*	*305*	*0.2926*	*3.37*	*0.05402*	*1.42*	*0.497*

Calculated Ages	$\frac{Pb^{207*}}{Pb^{206*}}$	**±2σ**	$\frac{Pb^{206*}}{U^{238}}$ **Age**	**(Ma)**	$\frac{Pb^{207*}}{U^{235}}$ **Age**	**±2σ (Ma)**	$\frac{Pb^{207*}}{Pb^{206*}}$ **Age**	**±2σ (Ma)**
Sample		**(pct)**						
SFM-1V3	0.09226	0.42	1336	9	1390	12	1473	8
SFM-1V1a	0.09248	0.87	1441	9	1456	16	1477	17
SFM-1V4	*0.03929*	*2.94*	*339*	*5*	*261*	*9*	*1*	*0*

Table 2: Ar-Ar isotopic data associated with spectrums shown in Figure 7a-e.

Diabase Groundmass, 1.40 mg, J = 0.006758 ± 0.76%												
4 amu discrimination = 1.0544 ± 0.49%, 40/39K = 0.00486 ± 65.19%, 36/37Ca = 0.000243 ± 24.65%, 39/37Ca = 0.000605 ± 14.11%												
step	**T (C)**	**t (min.)**	**36Ar**	**37Ar**	**38Ar**	**39Ar**	**40Ar**	**%40Ar***	**% 39Ar rlsd**	**40Ar*/39ArK**	**Age (Ma)**	**1s.d.**
1	570	12	0.525	0.021	0.121	0.774	200.222	33.0	1.1	71.778758	713.46	10.62
2	650	12	0.238	0.022	0.074	1.267	169.996	79.3	1.8	82.184846	796.93	7.17
3	700	12	0.222	0.027	0.093	2.020	259.472	89.8	2.9	98.516104	920.60	7.38
4	750	12	0.232	0.023	0.135	3.369	463.01	94.0	4.9	110.380275	1005.41	7.93
5	800	12	0.246	0.026	0.213	7.419	1100.02	97.2	10.7	140.304958	1203.13	8.70
6	850	12	0.253	0.030	0.368	13.564	2128.65	98.5	19.6	153.167624	1281.88	9.12
7	910	12	0.240	0.030	0.403	15.787	2296.35	98.8	22.8	142.558483	1217.18	8.80
8	970	12	0.225	0.026	0.366	11.917	1705.17	98.6	17.2	139.120142	1195.70	8.62
9	1030	12	0.221	0.022	0.212	5.073	712.352	97.1	7.3	129.981442	1137.34	8.42
10	1090	12	0.197	0.027	0.235	2.684	354.641	95.1	3.9	112.583086	1020.73	7.84
11	1150	12	0.202	0.025	0.347	2.469	341.423	94.9	3.6	116.468379	1047.43	8.11
12	1220	12	0.196	0.025	0.101	1.238	200.556	91.5	1.8	118.759615	1062.99	8.62
13	1290	12	0.202	0.027	0.058	0.872	161.372	97.4	1.3	121.286433	1080.00	9.07
14	1400	12	0.207	0.022	0.063	0.846	161.8	89.7	1.2	126.307640	1113.34	9.25
							Cumulative %39Ar rlsd =		100.0	Total gas age =	1167.13	7.94
note: isotope beams in mV, rlsd = released, error in age includes J error, all errors 1 sigma										No plateau		
(36Ar through 40Ar are measured beam intensities, corrected for decay for the age calculations)										No isochron		

Silvermines Granite-At the contact with diabase, K-spar, 4.90 mg, J = 0.00663 ± 0.74%												
4 amu discrimination = 1.0473 ± 0.40%, 40/39K = 0.00486 ± 65.19%, 36/37Ca = 0.000243 ± 24.65%, 39/37Ca = 0.000605 ± 14.11%												
step	T (C)	t (min.)	36Ar	37Ar	38Ar	39Ar	40Ar	%40Ar*	% 39Ar rlsd	40Ar*/39ArK	Age (Ma)	1s.d.
1	448	18	1.343	0.026	1.124	15.167	3169.26	89.8	3.9	186.497078	1452.10	8.52
2	473	18	0.298	0.022	0.207	8.838	1295.26	97.8	2.3	138.849570	1177.38	7.32
3	473	43	0.455	0.020	0.221	9.109	1446.45	100.0	2.4	144.538439	1212.47	7.42
4	514	18	0.296	0.022	0.373	14.795	2944.81	98.9	3.8	165.334498	1335.22	7.89
5	514	43	0.439	0.016	0.269	13.954	2282.93	100.0	3.6	154.987868	1275.19	7.67
6	555	18	0.349	0.027	0.475	16.456	2965.22	98.6	4.3	176.347311	1396.99	8.14
7	555	43	0.425	0.020	0.304	16.430	2854.46	100.0	4.3	164.682191	1331.49	7.86
8	596	18	0.371	0.018	0.440	16.394	2906.29	98.3	4.3	173.000428	1378.44	8.13
9	596	43	0.420	0.023	0.287	15.017	2550.43	100.0	3.9	148.409261	1235.96	7.47
10	638	18	0.295	0.027	0.275	11.034	1849.21	98.5	2.9	162.073387	1316.51	7.96
11	638	43	0.418	0.020	0.219	10.310	1664.75	100.0	2.7	149.118190	1240.23	7.50
12	679	19	0.243	0.021	0.166	7.493	1145.26	98.9	1.9	145.589931	1218.88	7.46
13	679	43	0.411	0.020	0.186	7.871	1148.08	100.0	2.0	128.928152	1114.51	7.03
14	720	19	0.234	0.024	0.148	5.793	784.98	98.7	1.5	125.843885	1094.51	6.96
15	720	43	0.408	0.026	0.168	6.099	806.445	100.0	1.6	109.727581	986.24	6.41
16	761	19	0.221	0.021	0.099	3.391	430.546	98.4	0.9	110.339947	990.47	6.54
17	761	43	0.391	0.023	0.132	3.932	512.56	99.9	1.0	94.534959	877.85	5.93
18	802	19	0.232	0.020	0.093	2.868	346.613	96.9	0.7	99.779792	916.01	6.12
19	843	19	0.286	0.025	0.144	4.458	510.584	94.7	1.2	97.986624	903.06	2.92
20	884	19	0.298	0.020	0.183	5.618	633.169	95.3	1.5	99.223925	912.01	6.17
21	910	19	0.250	0.019	0.138	4.597	533.947	97.1	1.2	102.368514	934.55	6.28
22	935	19	0.245	0.020	0.139	4.288	509.747	97.2	1.1	104.365072	948.72	6.26
23	961	19	0.253	0.024	0.161	4.670	546.338	97.0	1.2	103.271292	940.97	6.30
24	976	19	0.253	0.019	0.159	4.824	587.465	97.2	1.3	108.598163	978.40	6.40
25	1002	19	0.277	0.022	0.220	7.036	844.936	97.3	1.8	110.510393	991.65	6.63
26	1018	19	0.268	0.015	0.231	7.208	881.946	97.7	1.9	113.418453	1011.61	6.51
27	1033	19	0.277	0.022	0.253	7.295	889.098	97.4	1.9	112.710183	1006.77	6.53
28	1048	19	0.280	0.019	0.261	6.933	868.69	97.3	1.8	115.496090	1025.74	6.64
29	1064	19	0.284	0.019	0.288	6.981	918.067	97.3	1.8	121.695169	1067.25	6.80
30	1074	19	0.285	0.022	0.311	6.483	895.368	97.2	1.7	127.458553	1105.01	7.00
31	1084	19	0.304	0.026	0.329	6.315	893.061	96.5	1.6	129.633210	1119.05	7.00
32	1089	24	0.351	0.024	0.395	7.201	1052.29	97.4	1.9	133.887303	1146.21	7.26
33	1089	29	0.392	0.019	0.371	6.556	1008.97	98.1	1.7	138.843950	1177.35	7.25
34	1089	39	0.483	0.023	0.408	6.485	1061.88	99.3	1.7	144.694180	1213.42	7.52
35	1089	59	0.691	0.020	0.530	7.639	1319.75	100.0	2.0	148.290854	1235.24	7.62
36	1089	74	0.834	0.021	0.499	6.671	1253.39	100.0	1.7	151.558970	1254.85	7.63
37	1089	74	0.819	0.020	0.427	5.255	1046.66	100.0	1.4	152.605851	1261.08	7.80
38	1089	74	0.787	0.020	0.367	3.995	849.865	100.0	1.0	150.910330	1250.97	8.13
39	1089	74	0.750	0.020	0.288	2.594	637.908	99.9	0.7	149.668686	1243.54	7.99
40	1089	89	0.876	0.021	0.306	2.508	663.342	100.0	0.7	143.380740	1205.38	9.00
41	1089	119	1.173	0.023	0.372	2.740	791.365	100.0	0.7	138.631920	1176.03	8.53
42	1089	149	0.146	0.023	0.440	2.786	883.238	99.9	0.7	130.396626	1123.96	8.81
43	1141	20	0.252	0.022	0.162	1.324	327.547	95.3	0.3	196.789796	1506.33	10.00
44	1200	20	0.448	0.019	1.006	9.187	2090.02	96.7	2.4	216.407512	1605.37	8.93
45	1230	20	0.795	0.018	1.940	20.699	4600.57	96.4	5.4	214.013955	1593.57	8.91
46	1255	20	0.682	0.027	1.422	19.013	3719.81	96.4	4.9	187.806605	1459.09	8.41
47	1300	20	0.550	0.021	1.010	13.354	2557.51	96.2	3.5	182.136522	1428.63	8.37
48	1350	20	0.430	0.023	0.647	3.657	1323.3	95.4	0.9	332.268582	2100.07	10.52
49	1400	20	0.287	0.024	0.155	0.696	286.114	92.0	0.2	296.071306	1959.56	11.89
50	1500	20	0.368	0.025	0.298	1.519	512.604	91.0	0.4	271.387900	1857.06	10.21
								Cumulative %39Ar rlsd =	100.0	Total gas age =	1258.96	8.62
note: isotope beams in mV, rlsd = released, error in age includes J error, all errors 1 sigma												
(36Ar through 40Ar are measured beam intensities, corrected for decay for the age calculations)												

Silvermines Granite-At Contact with Diabase, Amphibole, 3.30 mg, J = 0.006544 ± 0.91%												
4 amu discrimination = 1.0623 ± 0.30%, 40/39K = 0.0049 ± 65.19%, 36/37Ca = 0.000243 ± 24.65%, 39/37Ca = 0.000605 ± 14.11%												
step	**T (C)**	**t (min.)**	**36Ar**	**37Ar**	**38Ar**	**39Ar**	**40Ar**	**%40Ar***	**% 39Ar rlsd**	**40Ar*/39ArK**	**Age (Ma)**	**1s.d.**
1	850	12	1.756	0.042	3.581	158.322	17244.23	97.4	37.8	107.018714	957.65	7.37
2	950	12	0.276	0.022	0.785	50.289	2805.33	99.3	12.0	101.445142	918.53	7.20
3	990	12	0.228	0.023	0.407	20.320	1805.8	98.8	4.9	86.607004	810.04	6.46
4	1060	12	0.380	0.024	0.754	33.094	2805.33	97.7	7.9	82.429024	778.28	6.27
5	1130	12	0.314	0.024	1.115	48.901	4348.22	99.0	11.7	88.083689	821.14	6.55
6	1200	12	0.282	0.021	1.758	77.981	7813.21	99.6	18.6	100.289435	910.31	7.07
7	1250	12	0.184	0.019	0.375	16.595	1720.12	99.7	4.0	101.605858	919.67	7.13
8	1300	12	0.162	0.027	0.115	3.944	453.733	100.0	0.9	104.215396	938.08	7.35
9	1400	12	0.198	0.025	0.208	9.372	1020.64	99.5	2.2	103.825893	935.34	7.23
							Cumulative %39Ar rlsd =		100.0	Total gas age =	904.82	8.20
note: isotope beams in mV, rlsd = released, error in age includes J error, all errors 1 sigma										No plateau		
(36Ar through 40Ar are measured beam intensities, corrected for decay for the age calculations)										No isochron		

Silvermines Granite-~30 ft. from contact with diabase, Biotite, 4.30 mg, J = 0.006687 ± 0.70%												
4 amu discrimination = 1.0623 ± 0.30%, 40/39K = 0.00486 ± 65.19%, 36/37Ca = 0.000243 ± 24.65%, 39/37Ca = 0.000605 ± 14.11%												
step	**T (C)**	**t (min.)**	**36Ar**	**37Ar**	**38Ar**	**39Ar**	**40Ar**	**%40Ar***	**% 39Ar rlsd**	**40Ar*/39ArK**	**Age (Ma)**	**1s.d.**
1	600	12	3.729	0.022	1.023	2.018	1253.65	86.2	2.9	125.338936	1098.24	7.13
2	665	12	1.580	0.022	1.037	8.695	873.324	52.1	12.6	50.473544	524.65	4.32
3	725	12	7.217	0.016	2.074	12.038	3020.24	33.9	17.4	84.860932	810.86	7.72
4	775	12	0.523	0.017	0.367	4.704	740.252	84.9	6.8	127.437234	1111.96	7.57
5	820	12	0.336	0.022	0.237	2.981	549.508	89.5	4.3	154.028821	1277.34	7.66
6	860	12	0.265	0.019	0.144	1.714	299.769	86.9	2.5	132.185023	1142.62	7.40
7	900	12	0.306	0.024	0.151	1.492	275.889	80.7	2.2	127.933428	1115.19	7.76
8	940	12	0.373	0.027	0.272	2.300	459.181	85.0	3.3	155.393523	1285.44	8.49
9	980	12	0.349	0.026	0.289	1.921	413.294	85.0	2.8	165.424975	1343.83	7.84
10	1030	12	0.465	0.022	0.523	3.177	610.936	84.5	4.6	152.654815	1269.16	7.96
11	1065	12	0.633	0.027	1.457	7.037	1235.55	88.7	10.2	151.969478	1265.06	7.51
12	1100	12	0.303	0.025	0.888	4.981	818.071	94.5	7.2	148.573635	1244.63	7.36
13	1160	12	0.307	0.028	1.115	6.582	1059.03	96.1	9.5	149.358596	1249.37	7.28
14	1230	12	0.284	0.025	0.883	6.704	989.138	96.5	9.7	137.058196	1173.56	7.02
15	1400	12	0.379	0.019	0.674	2.712	553.934	89.0	3.9	166.004089	1347.14	7.77
							Cumulative %39Ar rlsd =		100.0	Total gas age =	1065.97	7.78
note: isotope beams in mV, rlsd = released, error in age includes J error, all errors 1 sigma										No plateau		
(36Ar through 40Ar are measured beam intensities, corrected for decay for the age calculations)										No isochron		

Silvermines Granite-30ft from contact with diabase, K-spar, 3.30 mg, J = 0.006751 ± 0.75%												
4 amu discrimination = 1.0473 ± 0.40%, 40/39K = 0.00486 ± 65.19%, 36/37Ca = 0.000243 ± 24.65%, 39/37Ca = 0.000605 ± 14.11%												
step	T (C)	t (min.)	36Ar	37Ar	38Ar	39Ar	40Ar	%40Ar*	% 39Ar rlsd	40Ar*/39ArK	Age (Ma)	1s.d.
1	448	18	1.390	0.046	2.930	17.885	22231.15	98.5	0.9	1235.408581	4030.91	13.74
2	473	18	0.268	0.018	0.206	6.638	964.776	97.9	0.3	135.775712	1173.67	7.93
3	473	43	0.427	0.025	0.213	6.502	848.650	100.0	0.3	109.488769	998.38	6.55
4	514	18	0.347	0.013	1.110	22.820	8541.09	99.5	1.1	374.331745	2274.00	10.97
5	514	43	0.400	0.021	0.205	7.709	786.916	86.1	0.4	72.529618	719.00	5.24
6	555	18	0.351	0.019	1.061	26.285	6626.30	99.4	1.3	251.260514	1789.40	9.61
7	555	43	0.395	0.024	0.213	8.968	826.986	100.0	0.4	76.937187	754.68	5.23
8	596	18	0.313	0.020	0.634	20.471	3976.78	99.2	1.0	192.231036	1500.87	8.76
9	596	43	0.414	0.021	0.201	8.771	794.657	100.0	0.4	74.936987	738.57	5.38
10	638	18	0.369	0.018	0.372	12.826	1850.44	97.4	0.6	137.897034	1187.10	7.37
11	638	43	0.419	0.025	0.213	9.386	811.294	100.0	0.5	71.819411	713.18	5.12
12	679	19	0.252	0.017	0.281	12.817	1455.28	99.0	0.6	109.377983	997.60	6.53
13	679	43	0.412	0.023	0.259	12.822	1061.99	100.0	0.6	72.349041	717.52	5.04
14	720	19	0.282	0.020	0.359	17.385	1710.57	98.6	0.8	95.004828	893.99	6.00
15	720	43	0.432	0.020	0.321	17.943	1401.44	100.0	0.9	72.526071	718.97	5.05
16	761	19	0.253	0.023	0.258	14.056	1138.84	98.6	0.7	76.944672	754.74	5.27
17	761	43	0.413	0.018	0.323	18.073	1438.37	100.0	0.9	72.392063	717.87	5.01
18	802	19	0.241	0.028	0.245	14.393	1149.60	99.0	0.7	76.134466	748.23	5.20
19	843	19	0.279	0.026	0.369	21.887	1750.10	98.7	1.1	77.327502	757.80	5.27
20	884	19	0.284	0.016	0.452	26.348	2168.92	98.9	1.3	80.259303	781.11	5.36
21	910	19	0.257	0.023	0.431	23.912	2093.28	99.2	1.2	85.554290	822.46	5.58
22	935	19	0.276	0.018	0.538	28.046	2718.75	99.2	1.4	95.309998	896.25	5.97
23	961	19	0.283	0.023	0.732	36.358	3753.65	99.4	1.8	102.256791	947.01	6.23
24	976	19	0.294	0.022	0.851	42.410	4691.56	99.4	2.1	109.006286	995.00	6.47
25	1002	19	0.321	0.018	1.253	61.941	7007.08	99.5	3.0	112.976252	1022.64	6.64
26	1018	19	0.328	0.017	1.359	66.100	7570.07	99.5	3.2	114.454050	1032.82	6.64
27	1033	19	0.329	0.024	1.355	66.903	7650.07	99.5	3.2	114.284250	1031.65	6.63
28	1048	19	0.331	0.019	1.359	65.580	7522.05	99.5	3.2	114.606774	1033.87	6.64
29	1064	19	0.340	0.025	1.401	66.844	7765.59	99.5	3.2	116.086918	1044.00	6.75
30	1074	19	0.332	0.018	1.314	61.235	7178.52	99.5	3.0	117.059983	1050.64	6.72
31	1084	19	0.327	0.017	1.266	59.249	7074.90	99.5	2.9	119.238644	1065.40	6.81
32	1089	24	0.327	0.387	1.388	65.070	7896.36	99.8	3.2	121.300461	1079.26	6.89
33	1089	29	0.426	0.013	1.337	61.563	7540.52	99.6	3.0	121.940409	1083.54	6.89
34	1089	39	0.534	0.022	1.422	65.585	8141.38	99.7	3.2	123.268039	1092.38	7.00
35	1089	59	0.929	0.060	1.935	86.886	11021.50	99.4	4.2	125.267716	1105.63	6.99
36	1089	74	0.863	0.021	1.547	67.488	8625.20	100.0	3.3	125.867723	1109.58	6.99
37	1089	74	0.713	0.016	1.253	54.936	7100.59	100.0	2.7	126.058392	1110.84	7.00
38	1089	74	0.739	0.021	0.853	36.019	4767.63	100.0	1.7	126.751843	1115.39	7.02
39	1089	74	0.743	0.020	0.720	28.731	3842.59	100.0	1.4	126.338940	1112.68	7.02
40	1089	89	0.884	0.021	0.754	28.927	3942.50	100.0	1.4	127.088165	1117.60	7.04
41	1089	119	1.171	0.022	0.871	32.623	4493.03	100.0	1.6	126.409844	1113.15	7.06
42	1089	149	1.491	0.025	0.958	34.180	4798.27	100.0	1.7	126.488073	1113.66	7.17
43	1141	20	0.275	0.024	0.356	14.864	1981.34	99.0	0.7	129.623274	1134.14	7.16
44	1200	20	0.594	0.057	1.989	84.899	11063.17	99.0	4.1	129.833350	1135.51	7.18
45	1230	20	0.878	0.071	3.786	168.684	22245.93	99.2	8.2	131.924552	1149.03	7.22
46	1255	20	0.881	0.060	3.925	182.681	25169.35	99.2	8.8	137.998044	1187.74	7.35
47	1300	20	0.892	0.054	3.388	154.068	21438.77	99.2	7.5	139.114371	1194.76	7.40
48	1350	20	0.242	0.027	0.126	4.011	673.252	99.2	0.2	151.974340	1273.77	7.75
49	1400	20	0.239	0.020	0.121	3.450	494.651	99.0	0.2	124.530096	1100.75	7.04
50	1500	20	0.334	0.024	0.300	8.091	1183.81	97.3	0.4	135.952962	1174.79	7.44
							Cumulative %39Ar rlsd =		100.0	Total gas age =	1119.31	7.47
note: isotope beams in mV, rlsd = released, error in age includes J error, all errors 1 sigma												
(36Ar through 40Ar are measured beam intensities, corrected for decay for the age calculations)												